An academic exercise on layout optimization of pin-jointed frames

Fernandez Cabo, Jose L.
jose.fcabo@upm.es
Antuña Bernardo, Joaquín
joaquinfrancisco.antuna@upm.es

Key words: educational, layout optimization, minimum weight, frameworks, pin-jointed, conceptual design, structures.

Abstract

This article describes an academic exercise recently carried out in the *Escuela Técnica Superior de Arquitectura de Madrid,* within the course *La Estructura en el Proyecto Arquitectónico* (Structure in Architectural Project).

The goal was to work on the layout optimization of pin-jointed frames. The students had to design the layout of a structure with a set system of forces in equilibrium and within geometrical bounds. The students were helped by a script implemented in MATALB® in order to compute the volume of material (the primary objective function) and other derived parameters. This allowed students to focus their attention in the topic of learning, while at the same time the results of the exercise were more reliable.

Different solutions were analyzed as the basis of further discussion in the classroom. Theoretical concepts then arise naturally and are linked with their previous work, which make it easier to address abstract concepts and reinforce the learning process.

The exercise shows that the key parameter is slenderness (defined as the ratio between the span and the maximum depth of the framework). The scheme is less sensitive. Once the chords of the structure are designed with an adequate slenderness, it only remains to place the web elements with angles of around 45 degrees. For slenderness higher than approx. 8 to 10, the best design is a truss with parallel chords and diagonals between 30 and 60 degrees (better from 45 to 60 degrees). For slenderness lower than approx. 8 the arch is more efficient than a truss. This means that for typical frameworks, the skills of the designer are almost restricted to the election of the slenderness.

Built examples are finally reviewed in order to see how managing the different variables of an actual structure is a subtle question, one that cannot be detected in the previous theoretical exercise. Simplicity is crucial. Techniques such as prestressing notably increase efficiency.

The article also presents architectural masterpieces built in short and medium spans, sometimes made with low efficiency structural schemes. Any real problem is complex, and good solutions must manage all of the variables. Although structural efficiency does not guarantee architectural success, both of these are compatible.

1 Introduction

There are different approaches to teaching. But finally students learn only when they are committed to the process of learning, and exercises are crucial to get them involved in that process.

This article describes an academic exercise designed to teach the layout optimization of pin-jointed workframes. It was developed at the *Escuela Técnica Superior de Arquitectura de Madrid* (ETSAM) in the course *La Estructura en el Proyecto Arquitectónico* (Structure in Architectural Project).

This course addresses the coneptual design of structures. Theoretical concepts are combined with visual analysis of built structures. Experience has proven that the former is always difficult for students. The aim of this exercise was to facilitate the understanding of frame layout optimization. The use of a script implemented in MATALB® was crucial for undertaking the task with a reasonable amount of work and in a reliable manner.

The exercise encouraged fruitful discussion in classroom and to reinforce the knowledge of basic theoretical concepts. Only primary questions were dealt with, but in such a way that they would be part of the students' structural insight in the future.

Section 2 describes the exercise; Section 3 summarizes the theoretical basis used by the students in this topic; Section 4 shows the results; Section 5 discusses the results; Section 6 reviews built structures (an important question due to the simple assumptions used in the previous Sections) and Section 7 compiles conclusions. Appendix A lists the script of MATLAB® with additional comments.

2 The exercice

The exercise is summarized in the figure 1 . Data are: the set of forces in equilibrium, distributed along the line **ab** (kinematical conditions are therefore implicitly assumed); within a geometrical bound defined by the rectangle **abcd**.

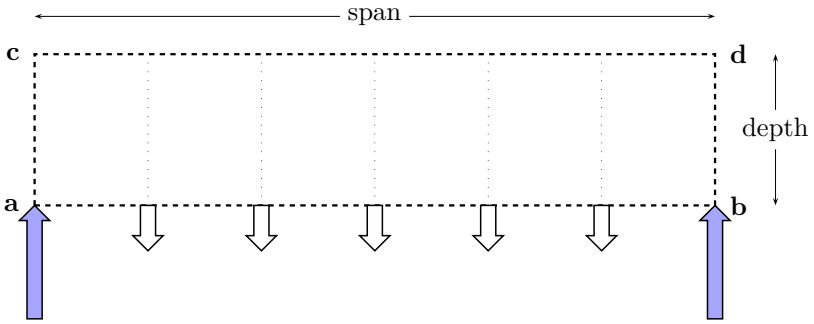

Figure 1: Description of the exercise: define a pin-jointed frame in equilibrium under a given system of forces in equilibrium along the line **ab** and constrained in its geometry by the rectangle **abcd**

The student must propose either a truss or a funicular layout, subject to the above conditions.

The set of forces corresponds to a typical problem in building structures; the problem of a simple supported structure with a continuous load. The division of a continuous load using five point loads is an interesting question to discuss in the classroom.

Proposals are limited to statically determinate trusses and funiculars layouts due to two main reasons. Firstly, most medium span structures and all long span ones are designed using workframes; they are easy to produce and to build, and they are usually more efficient than continuous structures (where over-sizing is in practice always present). Secondly, these structures are either statically determinate (for the trusses) or over-statically determinate (for funicular schemes), and therefore only equilibrium is needed to obtain the internal forces. I.e., neither compatibility nor

constitutive equations are required. This is quite convenient for saving time and, most importantly, to focusing students' attention on the layout of the structure instead of its size. It must be remembered that the course centres on the conceptual design of structures.

Internal forces were obtained using a script implemented in MATLAB® which is included in Appendix A, which is valid for 3D systems. The theoretical basis can be seen in a similar script, using MAPLE®, as described by Fernandez Cabo (2012). Once those variables were computed, all the other ones are easily derived (additional details are given in the next section).

3 Theoretical basis: the state of the art

Layout optimization is a mature and wide field. The approach used in this course follows the path laid down by Maxwell (1890) and Michell (1904) and widened by Prof. Ricardo Aroca Hernández-Ros for the case of workframes (Aroca, 1989/1990, 1992/1993, 2002/2011). This section summarizes key concepts of Aroca's work used in exercise.

The volume V of a pin-jointed frames structure, with only point loads at the nodes, can be computed by summing up the volume of the m members that form the structure:

$$V = \sum_{1}^{m} A_j L_j = \frac{1}{\sigma} \underbrace{\sum_{1}^{m} \mid N_j \mid L_j}_{W} \tag{1}$$

where A is the cross-section area, L is the length, σ is the allowable stress (a assumed constant for optimum sizing) and N is the internal force.

The *quantity of material* W is defined as:

$$W = \sum_{1}^{m} \mid N_j \mid L_j \tag{2}$$

The volume V of the structure is therefore proportional to W. When the structure is not statically indeterminate, W can be computed regardless of the sizing; i.e. regarding the material, which makes it possible to focus on the layout. For statically indeterminate ones, it is possible to assume a priori a stress distribution and therefore also to avoid preliminary sizing.

W can be calculated as the sum of the contribution of the members in tension W^+ and compression W^-:

$$W^+ = \sum \mid N_j^+ \mid L_j \tag{3}$$

$$W^- = \sum \mid N_j^- \mid L_j \tag{4}$$

And therefore

$$W = W^+ + W^- \tag{5}$$

Maxwell (1890) stated an important theorem: given a set for forces in equilibrium, for all layouts associated with that system the difference between the quantity of material in tension and compression is an invariant, and that constant is usually termed Maxwell's constant, k_M:

$$k_M = W^+ - W^- \tag{6}$$

On the other hand, as W computes a *work*, each individual component can be computed as a scalar product; which makes it possible to compute W as a sum of their horizontal and vertical components, W_x and W_y:

$$\underbrace{|\ N_j\ |\ L_j}_{W_i} = \underbrace{|\ N_{jx}\ |\ L_{jx}}_{W_{ix}} + \underbrace{|\ N_{jy}\ |\ L_{jy}}_{W_{iy}} \tag{7}$$

where sub-indexes x and y refer to horizontal and vertical components respectively.

As W is proportional to the volume of the structure,*its value measures the efficiency of a specific layout*; and this why it is a key parameter in all the theory of layout optimization. In general terms, for a horizontal span and a set of vertical forces (at is the case here) W is proportional to the total load P and the span L:

$$W = \mu PL \tag{8}$$

where μ *is constant, and its value therefore measures the efficiency of each layout, the smaller its value the greater the efficiency.* This is a typical equation in the literature of layout optimization.

For a specific weight ρ, dead load P_{DL} is:

$$P_{DL} = \rho V = \frac{\rho}{\sigma} W = \frac{1}{\sigma/\rho} \mu PL \tag{9}$$

The parameter σ/ρ has a physical meaning: the maximum height that a prism with a constant cross-section can reach under dead load. σ/ρ groups all terms referring to material, an important question. Table 1 shows typical values of parameter σ/ρ.

Material	σ/ρ (m)
Masonry	5,000
Reinforced concrete	300
Typical sawn timber	1,500
Normalised mild steel	2,100
Steel for cables	10,000
Carbon fibres	40,000

Table 1: Approximated values of (σ/ρ) for different materials.

One major breakthrough introduced by Prof. Ricardo Aroca was to clarify the parameter μ for the case of a set of vertical forces and a horizontal span, and bounding the geometrical changes to a set of affine transformations that keep the abscises of the nodes (in order to keep the span):

$$P_{DL} = \frac{1}{\sigma/\rho} \mu PL = \frac{1}{\sigma/\rho} PL \underbrace{k \left(\frac{\lambda}{\lambda_o} + \frac{\lambda_o}{\lambda} \right)}_{\mu} \tag{10}$$

where λ is the slenderness of the structure, defined by the span L divided by the maximum depth h, $\lambda = L/h$; λ_o the optimal slenderness, i.e. the slenderness associated with minimum weight (i.e. with minimum W); and k is a constant function of the scheme or topology of the structure.

Dead load is thereby expressed with an absolute and clear separation of the key variables in the problem:

$$P_{DL} = \underbrace{\frac{1}{\sigma/\rho}}_{MATERIAL} \quad \underbrace{P}_{LOAD} \underbrace{L}_{SPAN} \underbrace{k}_{SCHEME} \underbrace{\left(\frac{\lambda}{\lambda_o} + \frac{\lambda_o}{\lambda} \right)}_{SLENDERNESS} \tag{11}$$

where

$$W = PLk \left(\frac{\lambda}{\lambda_o} + \frac{\lambda_o}{\lambda} \right) \tag{12}$$

Scheme and slenderness, both geometrical variables, are therefore distinguished in the layout. Slenderness refers explicitly to only one variable, the ratio between the span and the maximum weight. But scheme implicitly assumes fixed abscises at

the nodes and also the ratio between their ordinates. The examples in Section 4 will clarify this important question.

The term $\frac{\lambda}{\lambda_o}$ is linked with W_x and the term $\frac{\lambda_o}{\lambda}$ with W_y; which means:

$$\begin{aligned} W_x &= PLk\left(\frac{\lambda}{\lambda_o}\right) \\ W_y &= PLk\left(\frac{\lambda_o}{\lambda}\right) \end{aligned} \tag{13}$$

For the optimal slenderness, $\lambda = \lambda_o$, these structural quantities are therefore equal:

$$W_{x,0} = W_{y,0} \tag{14}$$

The minimum structural quantity, W_0, for this scheme is:

$$W_0 = 2W_{x,0} = 2W_{y,0} = PL2k \tag{15}$$

For

$$\lambda = \lambda_o \rightarrow \mu_0 = 2k \tag{16}$$

Constant k and the optimal slenderness λ_0 can be computed using Eq. 13:

$$W_x W_y = P^2 L^2 k^2 \rightarrow k = \frac{\sqrt{W_x W_y}}{PL} \tag{17}$$

$$\frac{W_y}{W_x} = \frac{\lambda_0^2}{\lambda^2} \rightarrow \lambda_0 = \lambda\sqrt{\frac{W_y}{W_x}} \tag{18}$$

Finally let us return to Eq. 11. When a structure reaches its maximum span L_{max}, it can only bear dead load, i.e. $P = P_{DL}$, and therefore:

$$P_{DL} = \frac{1}{\sigma/\rho} P_{DL} L_{max} k\left(\frac{\lambda}{\lambda_o} + \frac{\lambda_o}{\lambda}\right) \rightarrow L_{max} = \frac{\sigma}{\lambda}\frac{1}{k\left(\frac{\lambda}{\lambda_o} + \frac{\lambda_o}{\lambda}\right)} \tag{19}$$

Notice that $k(\lambda/\lambda_0 + \lambda_0/\lambda) = \mu$ (see Eq. 8) (this represents the quantity of material per unit of load and span $\mu = W/(PL)$) and therefore:

$$L_{max} = \frac{\sigma}{\rho}\frac{1}{\mu} \tag{20}$$

The previous equation can be derived at the limit state $L = L_{max}$ from Eq. 8, as was done in Eq. 18. It can be used for cases where an affine transformation does not lead to a structure, and therefore Eq. 10 is not longer valid. But it must be applied for each individual slenderness.

Buckling of the members can be considered in the script of MATLAB® assuming a constant mean value as buckling coefficient (termed *omega* in the script) for all the members in compression. In these cases, compression forces are multiplied for that value in order to compute the increase of material due to local buckling. General buckling was not studied in this exercise, and parametrical study related with *omega* is not developed here.

4 Results

A MATLAB® script (see Appendix-A) computes the values of: W (Eq. 2), W_x (Eq. 3), W_y (Eq. 4), (and W_z for a 3D case), k (Eq. 17), λ_0 (Eq. 13), L_{max} (Eq. 19 and Eq. 20). It was run for each type considering four values of slenderness: $\lambda = \lambda_0$; $\lambda = 2\lambda_0$; $\lambda = 12$ and $\lambda = 24$. Buckling is not considered. Further explanations about it will be given in the next Section.

Tables 2 to 26 summarise the results. Only typical building construction solutions were studied by the students.

The four values of slenderness were selected following the criteria below. Optimum value, $\lambda = \lambda_0$, without considering buckling and other factors such as wind load, the cost of cladding, etc. Doubling the slenderness, $\lambda = 2\lambda_0$, the increase of weight only amounts to 25%:

$$\frac{\left(\frac{\lambda=2\lambda_o}{\lambda_o} + \frac{\lambda_o}{\lambda=2\lambda_o}\right)}{\left(\frac{\lambda=\lambda_o}{\lambda_o} + \frac{\lambda_o}{\lambda=\lambda_o}\right)} = \frac{2,5}{2} = 1,25 \tag{21}$$

As buckling and other factors are not considered, the value of $\lambda = 2\lambda_0$ is in fact closer to the actual optimum slenderness, which agrees with what can be seen in medium and long span built structures.

The other two recorded cases are $\lambda = 12$ and $\lambda = 24$.

For parallel chord trusses, diagonals at approx. 45 degrees and constant sizing for chords and diagonals (i.e. with sizing for the maximum forces at those elements), and an allowable longitudinal strain of $\epsilon = 0,8 \cdot 10^{-3}$; $\lambda = 12$ leads to a maximum relative deflection of approx. 1/300; which uses to be a more than reasonable value for a roof. Roughly speaking, typical simple supported roof trusses with $\lambda = 12$ do not present stiffness problems. For medium and long span solutions typical slenderness is $2\lambda_0 = \lambda = 12$. This offers a better efficiency in strength.

$\lambda = 24$ leads to solutions where the stiffness control requires over-sizing, and this is often assumed, especially in secondary members. It can be considered to be approx. the upper limit for a simple supported frame.

The value of μ (see Eq. 8 and Eq. 16) is recorded in the results, as are μ_x and μ_y, corresponding to W_x and W_y respectively. This is useful to see how for $\lambda > 12$, μ_y and therefore W_y is negligible. It is also illustrative to confirm Eq. 15 for $\lambda = \lambda_0$; and also to see how $W_x = W_y$ for $\lambda = \lambda_0$ (see Eq. 15). The increase of weight from $\lambda = 12$ to $\lambda = 24$ is approximately proportional to the increase in slenderness. This is because the value of λ/λ_0, related to W_x is predominant (the term λ/λ_0, related to W_y, almost vanishes from approximately $\lambda > 8$).

Tables included in the figures below explicitly compute the quantity of material for the four analyzed values of slenderness.

The script plots the layout to scale. It is important that the student were able to see the exact proportion of all cases, so that they could store them in their visual memory. The figures in this section are also drawn to scale for the same reason.

L_{max} is obtained from (Eq. 19),and it is a theoretical upper bound. For an actual problem, where many other variables are considered, the maximum actual span according to experimental data is around 20% of that limit. This value is recorded for the case of normalised mild steel.

$\lambda_0 = 3.13 \quad k = 0.765$			for steel with (σ/ρ)=2100 m
λ	$\mu(\mu_x/\mu_y)$	L_{max}	$0.2L_{max}$ (m)
$= \lambda_0$	1.52(0.76/=)	$(\sigma/\rho)/1.52$	276
$= 2\lambda_0$	1.91(1.53/0.38)	$(\sigma/\rho)/1.91$	219
12	3.13(2.93/0.20)	$(\sigma/\rho)/3.13$	134
24	5.97(5.87/0.10)	$(\sigma/\rho)/5.97$	70

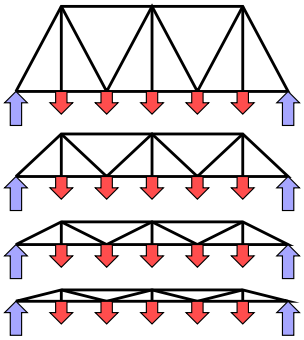

Table 2: Results for type #1.

$\lambda_0 = 2.69 \quad k = 0.7416$			for steel with (σ/ρ)=2100 m
λ	$\mu(\mu_x/\mu_y)$	L_{max}	$0.2L_{max}$ (m)
$= \lambda_0$	1.48(0.74/=)	$(\sigma/\rho)/1.48$	283
$= 2\lambda_0$	1.85(1.49/0.37)	$(\sigma/\rho)/1.85$	227
12	3.47(3.30/0.17)	$(\sigma/\rho)/3.47$	121
24	6.68(6.60/0.08)	$(\sigma/\rho)/6.68$	63

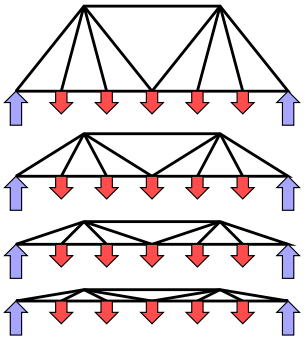

Table 3: Results for type #2.

$\lambda_0 = 2.1214 \quad k = 1.4142$			for steel with (σ/ρ)=2100 m
λ	$\mu(\mu_x/\mu_y)$	L_{max}	$0.2L_{max}$ (m)
$= \lambda_0$	2.83(1.41/=)	$(\sigma/\rho)/2.83$	149
$= 2\lambda_0$	3.54(2.83/0.71)	$(\sigma/\rho)/3.54$	119
12	8.25(8.0/0.25)	$(\sigma/\rho)/8.25$	51
24	16.12(16/0.12)	$(\sigma/\rho)/16.1$	26

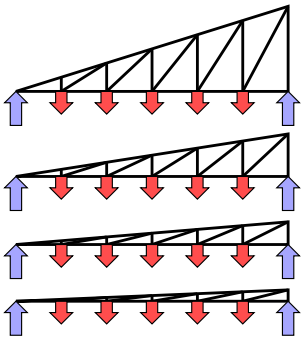

Table 4: Results for type #3.

$\lambda_0 = 2.5715 \quad k = 1.0874$			for steel with (σ/ρ)=2100 m
λ	$\mu(\mu_x/\mu_y)$	L_{max}	$0.2L_{max}$ (m)
$= \lambda_0$	2.17(1.09/=)	$(\sigma/\rho)/2.17$	193
$= 2\lambda_0$	2.72(2.17/0.54)	$(\sigma/\rho)/2.72$	155
12	5.32(5.07/0.23)	$(\sigma/\rho)/5.32$	79
24	10.3(10.2/0.12)	$(\sigma/\rho)/10.3$	41

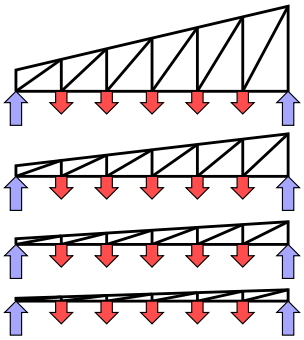

Table 5: Results for type #4.

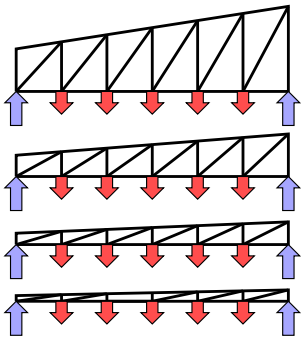

$\lambda_0 = 2.953 \quad k = 0.978$			for steel with (σ/ρ)=2100 m
λ	$\mu(\mu_x/\mu_y)$	L_{max}	$0.2L_{max}$ (m)
$= \lambda_0$	1.93(0.97/=)	$(\sigma/\rho)/1.93$	217
$= 2\lambda_0$	2.44(1.96/0.49)	$(\sigma/\rho)/2.44$	172
12	4.22(3.98/0.24)	$(\sigma/\rho)/4.22$	100
24	8.07(7.95/0.12)	$(\sigma/\rho)/8.07$	52

Table 6: Results for type #5.

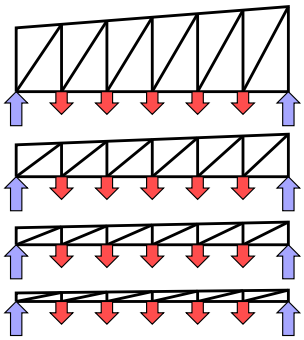

$\lambda_0 = 3.397 \quad k = 0.9518$			for steel with (σ/ρ)=2100 m
λ	$\mu(\mu_x/\mu_y)$	L_{max}	$0.2L_{max}$ (m)
$= \lambda_0$	1.90(0.95/=)	$(\sigma/\rho)/1.90$	221
$= 2\lambda_0$	2.38(1.90/0.48)	$(\sigma/\rho)/2.38$	177
12	3.63(3.36/0.27)	$(\sigma/\rho)/3.63$	116
24	6.86(6.72/0.13)	$(\sigma/\rho)/6.86$	61

Table 7: Results for type #6.

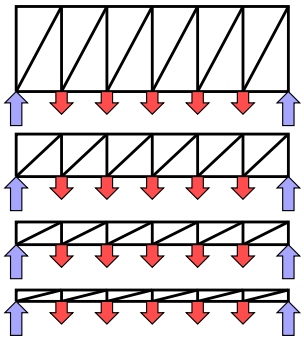

$\lambda_0 = 3.8376 \quad k = 0.9381$			for steel with (σ/ρ)=2100 m
λ	$\mu(\mu_x/\mu_y)$	L_{max}	$0.2L_{max}$ (m)
$= \lambda_0$	1.88(0.94/=)	$(\sigma/\rho)/1.88$	224
$= 2\lambda_0$	2.34(1.88/0.47)	$(\sigma/\rho)/2.34$	197
12	3.23(2.93/0.30)	$(\sigma/\rho)/3.23$	130
24	6.02(5.87/0.15)	$(\sigma/\rho)/6.02$	70

Table 8: Results for type #7.

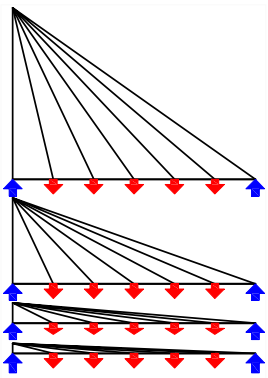

$\lambda_0 = 1.4142 \quad k = 1.4142$			for steel with (σ/ρ)=2100 m
λ	$\mu(\mu_x/\mu_y)$	L_{max}	$0.2L_{max}$ (m)
$= \lambda_0$	2.83(0.76/=)	$(\sigma/\rho)/2.83$	149
$= 2\lambda_0$	3.54(2.87/0.71)	$(\sigma/\rho)/3.54$	119
12	12.17(12/0.17)	$(\sigma/\rho)/12.2$	35
24	24.08(24/0.08)	$(\sigma/\rho)/24.1$	17

Table 9: Results for type #8.

$\lambda_0 = 1.789 \quad k = 1.118$			for steel with (σ/ρ)=2100 m
λ	$\mu(\mu_x/\mu_y)$	L_{max}	$0.2L_{max}$ (m)
$= \lambda_0$	2.24(1.12/=)	$(\sigma/\rho)/2.24$	188
$= 2\lambda_0$	2.80(2.24/0.56)	$(\sigma/\rho)/2.80$	150
12	7.67(7.50/0.17)	$(\sigma/\rho)/7.67$	55
24	15.08(15/0.08)	$(\sigma/\rho)/15.08$	28

Table 10: Results for type #9.

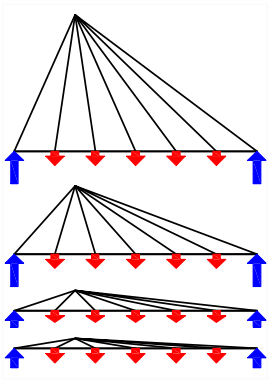

$\lambda_0 = 2 \quad k = 1$			for steel with (σ/ρ)=2100 m
λ	$\mu(\mu_x/\mu_y)$	L_{max}	$0.2L_{max}$ (m)
$= \lambda_0$	2(1/=)	$(\sigma/\rho)/2$	210
$= 2\lambda_0$	2.5(2/0.5)	$(\sigma/\rho)/2.5$	168
12	6.17(6.00/0.17)	$(\sigma/\rho)/6.17$	68
24	12.08(12/0.08)	$(\sigma/\rho)/12.08$	35

Table 11: Results for type #10.

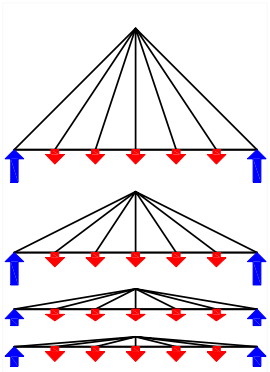

$\lambda_0 = 2 \quad k = 1$			for steel with (σ/ρ)=2100 m
λ	$\mu(\mu_x/\mu_y)$	L_{max}	$0.2L_{max}$ (m)
$= \lambda_0$	2(1/=)	$(\sigma/\rho)/2$	210
$= 2\lambda_0$	2.5(2.00/0.50)	$(\sigma/\rho)/2.5$	168
12	6.17(6.00/0.17)	$(\sigma/\rho)/6.17$	68
24	12.08(12/0.08)	$(\sigma/\rho)/5.42$	35

Table 12: Results for type #11.

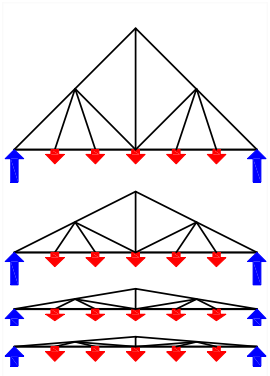

$\lambda_0 = 1.8619 \quad k = 0.9309$			for steel with (σ/ρ)=2100 m
λ	$\mu(\mu_x/\mu_y)$	L_{max}	$0.2L_{max}$ (m)
$= \lambda_0$	1.86(0.93/=)	$(\sigma/\rho)/1.86$	226
$= 2\lambda_0$	2.33(1.87/0.47)	$(\sigma/\rho)/2.33$	180
12	6.14(6/0.14)	$(\sigma/\rho)/6.14$	68
24	12.07(12/0.07)	$(\sigma/\rho)/12.07$	35

Table 13: Results for type #12.

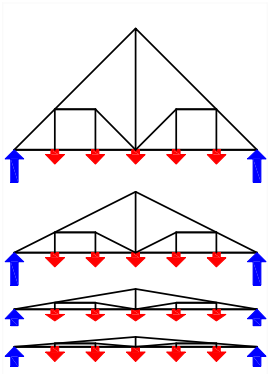

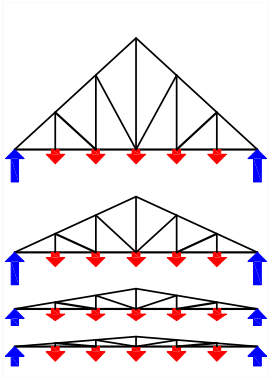

$\lambda_0 = 2.2039 \quad k = 1.0285$			for steel with (σ/ρ)=2100 m
λ	$\mu(\mu_x/\mu_y)$	L_{max}	$0.2L_{max}$ (m)
$= \lambda_0$	2.06(1.03/=)	$(\sigma/\rho)/2.06$	204
$= 2\lambda_0$	1.71(1.37/0.34)	$(\sigma/\rho)/1.71$	163
12	5.79(5.60/0.19)	$(\sigma/\rho)/5.79$	73
24	11.29(11.2/0.09)	$(\sigma/\rho)/11.3$	37

Table 14: Results for type #13.

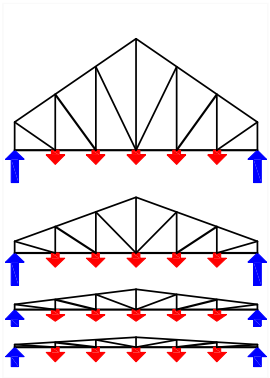

$\lambda_0 = 2.2206 \quad k = 0.7731$			for steel with (σ/ρ)=2100 m
λ	$\mu(\mu_x/\mu_y)$	L_{max}	$0.2L_{max}$ (m)
$= \lambda_0$	1.55(0.77/=)	$(\sigma/\rho)/1.55$	272
$= 2\lambda_0$	1.93(1.55/0.39)	$(\sigma/\rho)/1.93$	217
12	4.32(4.18/0.14)	$(\sigma/\rho)/4.32$	97
24	8.43(8.36/0.07)	$(\sigma/\rho)/8.43$	50

Table 15: Results for type #14.

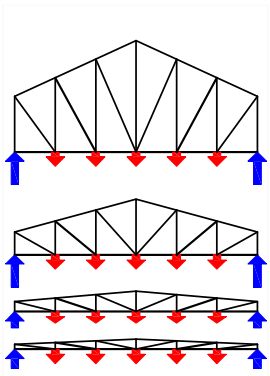

$\lambda_0 = 2.5462 \quad k = 0.7554$			for steel with (σ/ρ)=2100 m
λ	$\mu(\mu_x/\mu_y)$	L_{max}	$0.2L_{max}$ (m)
$= \lambda_0$	1.56(0.78/=)	$(\sigma/\rho)/1.56$	270
$= 2\lambda_0$	1.89(1.51/0.38)	$(\sigma/\rho)/1.89$	222
12	3.72(3.56/0.16)	$(\sigma/\rho)/3.72$	113
24	7.20(7.12/0.08)	$(\sigma/\rho)/7.20$	58

Table 16: Results for type #15.

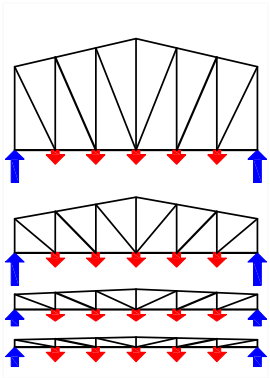

$\lambda_0 = 3.0789 \quad k = 0.8117$			for steel with (σ/ρ)=2100 m
λ	$\mu(\mu_x/\mu_y)$	L_{max}	$0.2L_{max}$ (m)
$= \lambda_0$	1.62(0.81/=)	$(\sigma/\rho)/1.62$	259
$= 2\lambda_0$	2.03(1.62/0.41)	$(\sigma/\rho)/2.03$	207
12	3.37(3.16/0.21)	$(\sigma/\rho)/3.37$	125
24	6.43(6.33/0.10)	$(\sigma/\rho)/6.43$	65

Table 17: Results for type #16.

$\lambda_0 = 2.93 \quad k = 0.946$			for steel with (σ/ρ)=2100 m
λ	$\mu(\mu_x/\mu_y)$	L_{max}	$0.2L_{max}$ (m)
$= \lambda_0$	1.89(0.95/=)	$(\sigma/\rho)/1.89$	222
$= 2\lambda_0$	2.36(1.89/0.47)	$(\sigma/\rho)/2.36$	178
12	4.11(3.87/0.23)	$(\sigma/\rho)/4.11$	102
24	7.86(7.75/0.12)	$(\sigma/\rho)/7.86$	53

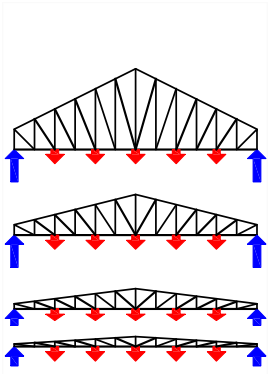

Table 18: Results for type #17.

$\lambda_0 = 2.93 \quad k = 0.946$			for steel with (σ/ρ)=2100 m
λ	$\mu(\mu_x/\mu_y)$	L_{max}	$0.2L_{max}$ (m)
$= \lambda_0$	1.97(0.98/=)	$(\sigma/\rho)/1.97$	213
$= 2\lambda_0$	2.46(1.97/0.49)	$(\sigma/\rho)/2.46$	171
12	3.56(3.26/0.30)	$(\sigma/\rho)/3.56$	118
24	6.67(6.52/0.15)	$(\sigma/\rho)/6.67$	63

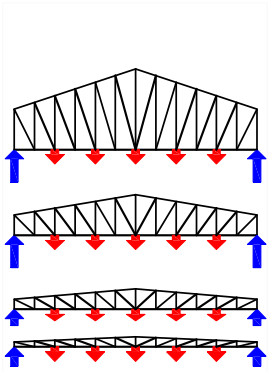

Table 19: Results for type #18.

$\lambda_0 = 5.316 \quad k = 1.0872$			for steel with (σ/ρ)=2100 m
λ	$\mu(\mu_x/\mu_y)$	L_{max}	$0.2L_{max}$ (m)
$= \lambda_0$	2.17(1.09/=)	$(\sigma/\rho)/2.17$	193
$= 2\lambda_0$	2.50(2.17/0.54)	$(\sigma/\rho)/2.50$	168
12	3.29(2.88/0.41)	$(\sigma/\rho)/$	3.29 128
24	5.96(5.76/0.21)	$(\sigma/\rho)/5.96$	70

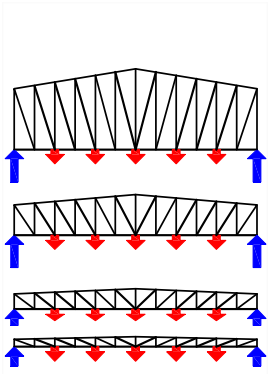

Table 20: Results for type #19.

$\lambda_0 = 5.728 \quad k = 1.257$			for steel with (σ/ρ)=2100 m
λ	$\mu(\mu_x/\mu_y)$	L_{max}	$0.2L_{max}$ (m)
$= \lambda_0$	2.51(1.26/=)	$(\sigma/\rho)/2.51$	167
$= 2\lambda_0$	3.14(2.51/0.63)	$(\sigma/\rho)/3.14$	134
12	3.23(2.63/0.60)	$(\sigma/\rho)/3.23$	130
24	5.57(5.27/0.30)	$(\sigma/\rho)/5.57$	75

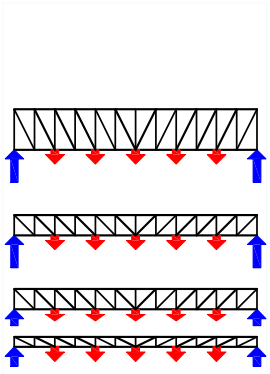

Table 21: Results for type #20.

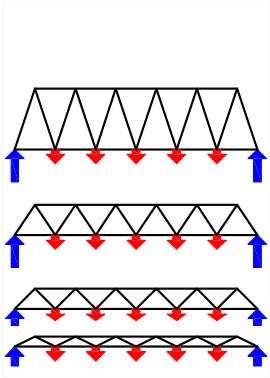

$\lambda_0 = 4.0503 \quad k = 0.8888$			for steel with (σ/ρ)=2100 m
λ	$\mu(\mu_x/\mu_y)$	L_{max}	$0.2L_{max}$ (m)
$= \lambda_0$	$1.78(0.89/=)$	$(\sigma/\rho)/1.78$	236
$= 2\lambda_0$	$2.22(1.78/0.44)$	$(\sigma/\rho)/2.22$	189
12	$2.93(2.63/0.30)$	$(\sigma/\rho)/2.93$	143
24	$5.42(5.27/0.15)$	$(\sigma/\rho)/5.42$	78

Table 22: Results for type #21.

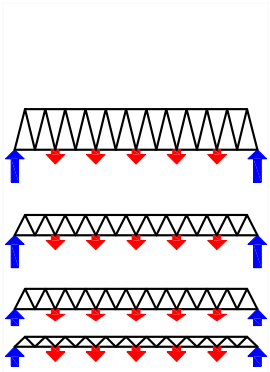

$\lambda_0 = 5.8985 \quad k = 1.2207$			for steel with (σ/ρ)=2100 m
λ	$\mu(\mu_x/\mu_y)$	L_{max}	$0.2L_{max}$ (m)
$= \lambda_0$	$2.44(1.22/=)$	$(\sigma/\rho)/2.44$	172
$= 2\lambda_0$	$3.05(2.44/0.61)$	$(\sigma/\rho)/3.05$	138
12	$3.08(2.48/0.60)$	$(\sigma/\rho)/3.08$	136
24	$5.27(4.97/0.30)$	$(\sigma/\rho)/5.27$	80

Table 23: Results for type #22.

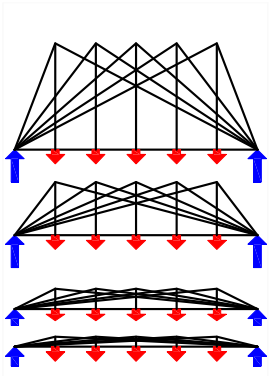

$\lambda_0 = 2.2678 \quad k = 0.8819$			for steel with (σ/ρ)=2100 m
λ	$\mu(\mu_x/\mu_y)$	L_{max}	$0.2L_{max}$ (m)
$= \lambda_0$	$1.76(0.88/=)$	$(\sigma/\rho)/1.76$	238
$= 2\lambda_0$	$2.20(1.76/0.44)$	$(\sigma/\rho)/2.20$	190
12	$4.83(4.67/0.17)$	$(\sigma/\rho)/4.83$	87
24	$9.42(9.33/0.08)$	$(\sigma/\rho)/9.42$	45

Table 24: Results for type #23.

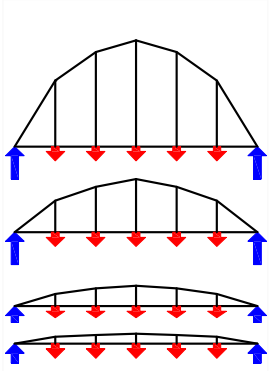

$\lambda_0 = 2.27 \quad k = 0.683$			for steel with (σ/ρ)=2100 m
λ	$\mu(\mu_x/\mu_y)$	L_{max}	$0.2L_{max}$ (m)
$= \lambda_0$	$1.37(0.68/=)$	$(\sigma/\rho)/1.37$	307
$= 2\lambda_0$	$1.71(1.37/0.34)$	$(\sigma/\rho)/1.71$	247
12	$3.73(3.60/0.34)$	$(\sigma/\rho)/3.73$	113
24	$7.26(7.20/0.06)$	$(\sigma/\rho)/7.26$	58

Table 25: Results for type #24.

$\lambda_0 = 2.4914 \quad k = 0.8028$			for steel with (σ/ρ)=2100 m
λ	$\mu(\mu_x/\mu_y)$	L_{max}	$0.2L_{max}$ (m)
$= \lambda_0$	1.61(0.80/=)	$(\sigma/\rho)/1.61$	262
$= 2\lambda_0$	2.01(1.61/0.4)	$(\sigma/\rho)/2.01$	209
12	4.03(3.87/0.17)	$(\sigma/\rho)/4.03$	104
24	7.82(7.73/0.08)	$(\sigma/\rho)/7.82$	54

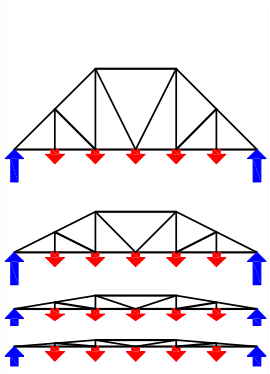

Table 26: Results for type #25.

5 Discussion

Fig. 2 plots the efficiency value μ (in ordinates) for the different types (with their reference number in abscises) and for the four analyzed values of slenderness.

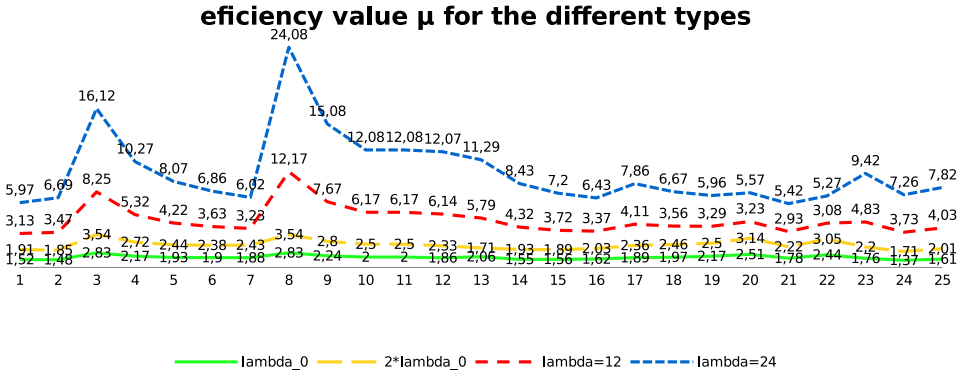

Figure 2: Efficiency μ (in ordinates) for each type (reference number in abscises) at the four analyzed values of slenderness

Fig. 3 plots the same results as Fig. 2 but removes the seven worst solutions; in particular types #3 and 8 to 13.

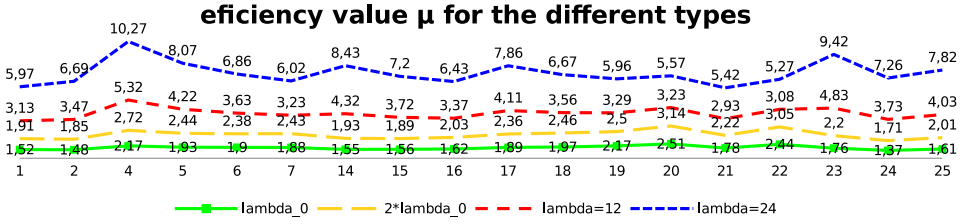

Figure 3: Efficiency μ (in ordinates) for each type (reference number in abscises) at the four analyzed degrees of slenderness when types #3, 8 to 13 are removed

Types #3, 8 to 13 are shown at Fig. 4.

They share the same problem: a low angle between the chord and the tie at one or both springs. This question is especially critical when slenderness is increased.

It is also useful to filter out the previous plot for optimum slenderness, as is shown in Fig. 5 and Fig. 6.

Types #4, #19, #20 and #22 (see Fig. 7) present intermediate efficiency. Although they are unlike the worst cases, they are still not as good as the best ones. Their problem is the angle between diagonals and chords, which should be between 30 and 60 degrees for a good efficiency.

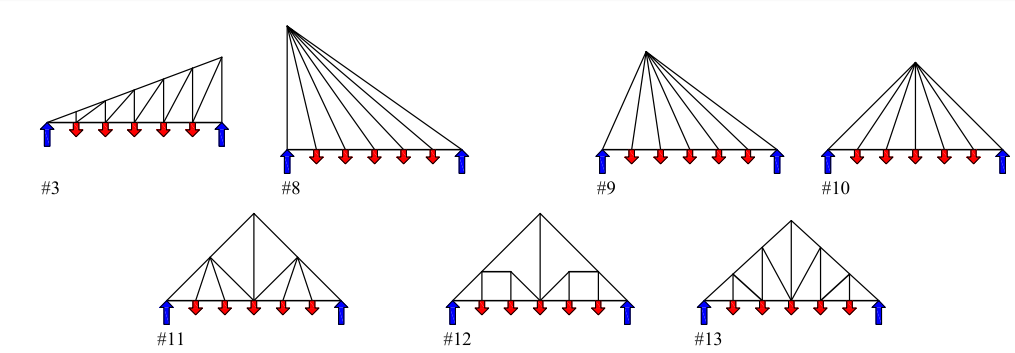

Figure 4: Types with the lowest efficiency removed from Fig. 2.

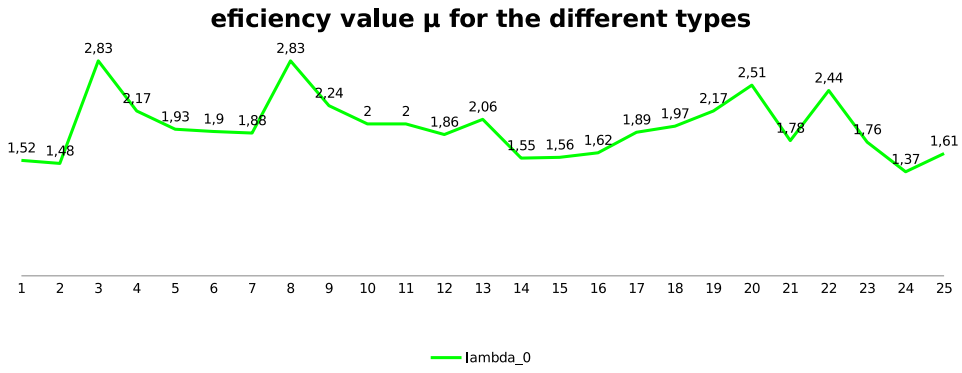

Figure 5: Efficiency μ (in ordinates) for each type (reference number in abscises) at optimum slenderness.

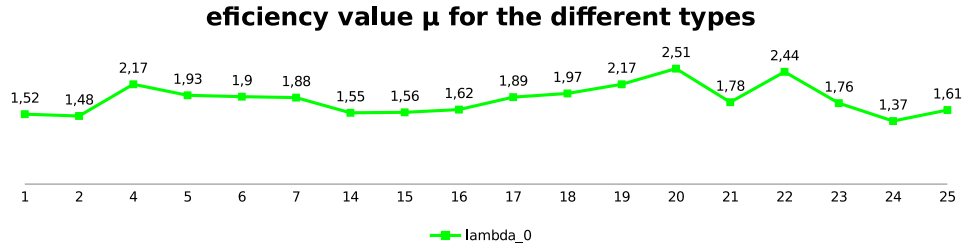

Figure 6: Efficiency μ (in ordinates) for each type (# in abscises) at optimum slenderness when types #3, 8 and 9 to 13 are removed.

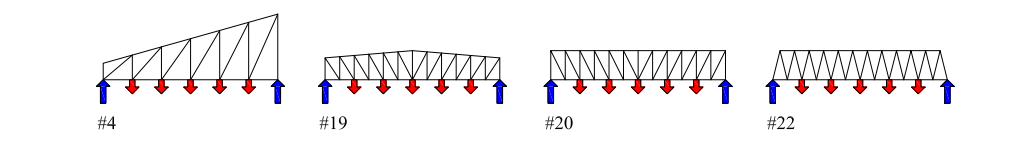

Figure 7: Types with an intermediate efficiency.

Removing types #4, #19, #20 and #22 would lead to a group of types with small differences.

The four best ones can be seen in Fig. 8. The differences between them are quite small, especially between the trusses.

Two important questions should be kept in mind here:

1. The quantity of material is just one component of the cost of a structure. De-

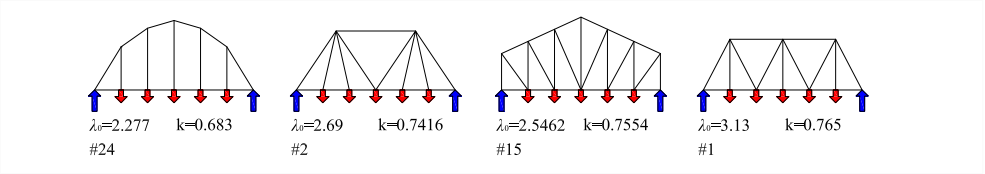

Figure 8: The best four types compared at their optimal slenderness.

pending on the material and type, its influence on cost varies, but can easily be only 1/3 to 1/4 of the total cost. This means that a less efficient scheme can be more than counterbalanced by the simplicity of its construction. This is a crucial question, as it notably reduces or modifies the theoretical differences between schemes. And this increases the key role of slenderness.

2. On other hand, cost is obviously not the only objective in architecture. The requirement uses to be to achieve a reasonable cost, but not an optimum one.

The differences shown in Fig. 2 can be therefore smaller or almost null in practice, especially when architectural values are added.

The range of efficiency for optimum slenderness is not kept when slenderness is increased. For example, let us compare type #24, the best one, with type #22. For a slenderness of $\lambda = 12$ type #22 is slightly better, and for $\lambda = 24$ is notably better. This is once again related to the low angle between the chord and tie at the springs in type #24 once slenderness is increased. Michell's theory (Michell, 1904) states that the sufficient condition for a minimum is that members at tension and compression intersect with angles of 90 degrees. The angles between these in type #22 stand at around 60 degrees, leading to a better solution.

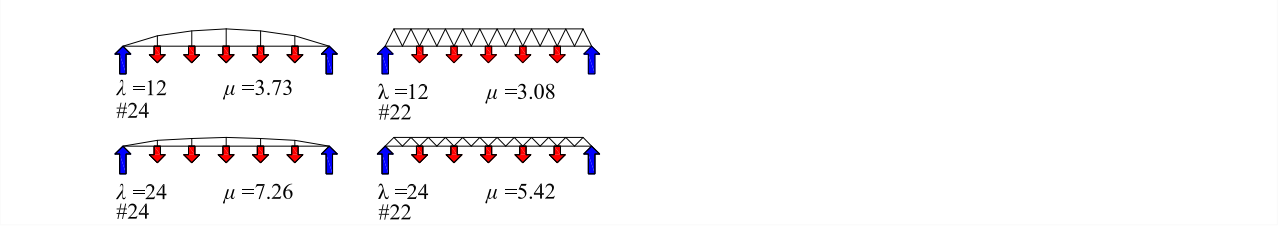

Figure 9: Comparison of the efficiency value μ between types #22 and #24 for slenderness of $\lambda = 12$ and $\lambda = 24$.

Last but not least, let us show how powerful the slenderness value is. The good schemes of type #24 and type #22 are now compared with the worst one, type #3, and another one which also has low efficiency, type #10. The comparison is made when the first two have $\lambda = 24$ and the second ones $\lambda = 2\lambda_0$. As can be seen in Fig. 10, proper slenderness counterbalances the lower quality of the scheme.

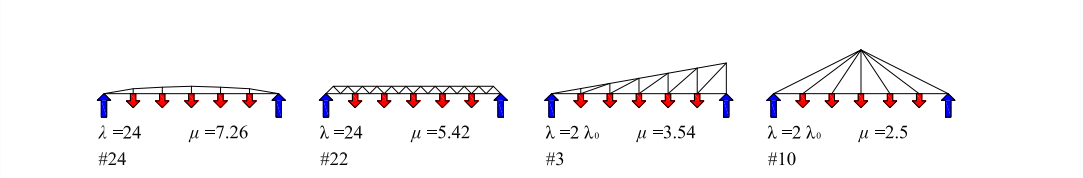

Figure 10: Comparison of the efficiency value μ between types #24 and #22 with types #3 and type #10 for a slenderness of $\lambda = 24$ and $\lambda = 2\lambda_0$ respectively.

Although other built examples will be shown in the next section, let us now depict two masterpieces basically built with types #3 and #10.

The first work is the chapel designed in 1957 by Heikki and Kaija Siren in Otaniemi (Fig. 11);corresponding to type #3, the worst scheme. The low slenderness of the

structure agrees with the need for natural light and a steep slope to prevent snow retention.

Figure 11: Chapel in Otaniemi, Finland. 1957. Architects: Heikki and Kaija Siren (© Ismael García Rios).

The second one is a design by Alvar Aalto for the city hall of Säynätsalo; corresponding approx. to type #10, but following a spatial arrangement, which is a logical and beautiful variation.

Figure 12: Roof structure in the City Hall of Säynätsalo, Finland, 1952. Architect: Alvar Aalto (© Jose L Fernandez Cabo.)

Seeing their slenderness it is now clear (with Fig. 10 in mind) that, while masterpieces from an architectural point of view, they additionally have a good efficiency value μ; and, even better, simplicity.

Good structural efficiency does not guarantee architectural success. But the two examples above prove that these good qualities are compatible.

It is usually possible to choose a proper slenderness in the case of roofs. As the majority of architectural spans are low or medium, designers have huge freedom in layout.

When a high slenderness is mandatory (as often happens), choosing types like #22, with parallel chords and diagonals at an angle to those chords of around 60 degrees is surely a good solution. But there are still other subtle decisions that can modify the range of good solutions, as will be shown in the next section. As an example, for short spans and high slenderness, commercial mild steel profiles are the best choice from the economic point of view, as readers can see in typical portal frames.

6 Review of structures: additional comments

The exercise was undertaken under simple assumptions. Actual structures must take many other variables into account. The revision of built examples can help place this exercise in a real context.

The exercise used a five point load scheme. Why? Because it can be considered to be a problem with continuous load. This is because the main scheme of a structure always corresponds to a limited group of point loads. How many depend on the

problem, but there tend to be just a few points in load schemes. Let us see some examples.

Figure 13: Highway overpass near Galapagar, Madrid, Spain.1966. Engineering: Carlos Fernández Casado, Leonardo Fernández Troyano and Javier Manterola Armisén (© Jose L Fernandez Cabo).

Fig. 13 shows a highway overpass close to Galapagar, Madrid, 48 m span. The deck is variable in depth from 0.6m at the abutments to 1.6m over the supports and 0.8m at the mid-span. See `http://www.cehopu.cedex.es/cfc/obras/FC-123.htm` for additional details. The general scheme is a funicular of three point loads. This shape allows a variable deck according to the variation of the secondary bending moments, which are crucial in this type of structure for strength and stability. 48m is a medium span for building structures.

Fig. 14 depicts the Infante D. Henrique bridge at Porto 280 m in span, the main scheme is again a funicular corresponding to just eight point loads. This design follows others by Robert Maillart and Christian Menn. The local slenderness for the arch elements is 186.5, which is really huge and unusual, and it is possible due to the relative local slenderness of the deck beam of 62.2. The arch has a slenderness of 11.2 (typical ones are usually from 5 to 8). The authors are aware of this challenge, but this high slenderness is assumed for aesthetic reasons.

Figure 14: Infante D. Henrique bridge, Porto, Portugal. Engineering: IDEAM and Adão da Fonseca & Associados, SA. 1999 - 2002. (© Jose L Fernandez Cabo).

Both previous examples show how typical schemes in bridges collect the actual load in a small number of point loads. Of course this is also the case in building structures. Fig. 15 shows the roof of the main train station in Zürich. The main scheme corresponds to arches with two point loads. The depth of the arch, and the main supports of the primary arches, means they are able to bear non-funicular loads.

On other hand, loads are variable in nature, and real optimization can only be achieved assuming different load cases. This reinforces the need to use simple main schemes.

Simplicity also explains why optimum structural schemes using Michell's principles, usually complex, are actually not optimum from a practical point of view.

Figure 15: Zürich main train station, Switzerland (© Jose L Fernandez Cabo).

Fig. 16 shows a crane used for the erection of a highway overpass, and one can expect an optimum design to be used for such a crane. And basically it is. It uses a scheme that is really efficient but also simple: good slenderness, a slope of the diagonals in the cantilever from 30 to 45 degrees, and a very efficient layout for anchoring the cantilever (Fig. 16b). A Michell layout for that corner is shown in Fig. 16c. It is clear that its complexity, and the consideration of buckling, actually makes it more expensive than the built solution. The depth of the secondary spatial truss elements makes it able to resist secondary internal forces.

Figure 16: Crane for the erection of a highway overpass in France. a) general view; b) detailed view of the corner; c) Michell's layout for the corner (© Jose L Fernandez Cabo).

Figure 17: (left) Bridge over the river Grijalva at Villahermosa, Tabasco, Mexico. 116m span. Engineering: Carlos Fernández Casado SL . 2001; © Carlos Fernández Casado SL; (right) Michell's layout for a double cantilever beam and continuous load.

Fig. 17 (left) is another bridge with tilt piles. The three-bay configuration makes possible a really efficient design and a practical approximation for Michell's layout of a double cantilever beam under continuous load (see Fig.17, right). Notice how the middle bay is longer than the sum of the lateral bays, in order to prevent the cables getting slack in a non-symmetrical load case (i.e. due to compression internal forces).

The previous example explains why the cable-stayed bridge in Fig.18 has the pile tilted forwards, thereby giving better angles between the cables and the deck (not less than approx. 30 degrees). Fig.18 (right) depicts a view of the deck that has to resist an important torque moment when only one lane is loaded. This again shows how the main layout is designed for the critical load pattern, almost never for all possible ones.

Figure 18: Bridge over N-VI highway close to Las Rozas, Madrid. 107 m span. 2006. Engineering: Arenas y Asociados. (© Jose L Fernandez Cabo).

Fig. 19 to Fig. 20 show also a example of a scheme with not so good efficiency but which use a slenderness $\lambda_0 < \lambda < 2 \cdot \lambda_0$ which finally gives rise to a rational structure.

Figure 19: Alvar Aalto. Roof structure at University of Jyväskyla, Finland. 1951-7. (© Jose L Fernandez Cabo).

Fig. 21 shows a bridge with a structure related to type #12. The good slenderness of the main scheme and the pre-stressed ties explains its good efficiency, and even more so if it is compare with the typical solution where only a concrete deck without external pre-stressed tendon is used.

Figure 20: (left) Roof of a sawmill of Valsaín, Segovia, Spain; (right) Vihantasalmi bridge, Finland. (© Jose L Fernandez Cabo).

The rules for designing efficient trusses were clarified, more empirically than theoretically, during the second half of the XIX century. Fig.22 shows an example designed by Owen Williams at 1930-32 for a Boots factory, a well-known masterpiece that was at the forefront of modern industrial architecture. It has a slenderness of approx. 9 and diagonals at angles around 45 degrees.

Figure 21: Bridge at Osomort, Barcelona, Spain. 13 bays with a 40m span. Engineering: Carlos Fernández Casado SL. 1994-95. (© Jose L Fernandez Cabo).

Figure 22: Boots factory. Designed by Owen Williams.1930-32. Nottingham, UK. (© Jose L Fernandez Cabo)Boots factory. Designed by Owen Williams.1930-32. Nottingham, UK. (© Jose L Fernandez Cabo).

Fig. 23 and Fig. 24 are recent examples of trusses for medium spans. These too follow the rules described above, and have a slenderness $\lambda_0 \leq \lambda \leq 2 \cdot \lambda_0$.

Figure 23: Cité des sciences et de l'industrie, Park de la Villette, Paris. (© Jose L Fernandez Cabo).

Figure 24: Media TIC, Barcelona. Architect: Enric Ruiz Geli; Structure: Agustí Obiols, BOMA. 2009. (© Jose L Fernandez Cabo).

Lenticular trusses were mainly used in the second half of the XIX century. Even when a good slenderness is used, a low angle between the chord and the tie at the springs reduces its efficiency. But that deficiency is balanced at the lenticular truss shown in Fig. 25 (122 m span) by the pre-stressed lower chord, where a high strength cable is used.

Figure 25: Exhibition hall at Hannover, Germany. 122m span. Architect: Gerkan, Marg und Partner. Structure: Schlaich Bergermann and partner. 1995. (© Jose L Fernandez Cabo).

Figure 26: Evenstand bridge, Norway. Engineering: Otto Kleppe (© Jose L Fernandez Cabo).

Fig. 26 shows a timber bridge related to type #15, one of the best ones, but using a curved upper chord. The upper chord is not polygonal but curved, to prevent using complex joints and paying just a small additional price for local stability. It is a good and typical solution. The arch is the most common historical type for medium spans (which at the time were long spans).

Kubel bridge (Fig. 27) near St. Gall, designed by Hans Grubenmann in 1780, is a type similar to #24, the best one. It has a single span of around 30m. The polygonal shape is explained by the use of sawn timber. A secondary truss-like system solves non-funicular loads. This is a brilliant piece of work.

Figure 27: Kubel bridge near St. Gall, Switzerland, 1780; designed by Hans Grubenmann (© Jose L Fernandez Cabo).

A similar modern example is shown in Fig. 28. This secondary element is built with bowstring type of approx. 10m in span made of timber and steel. The stiffness of the timber beams resolves non-funicular loads. This is a clean an efficient structure.

Figure 28: Ice Rink at Memmingen, Germany. Architect: Börner und Pasmann, Memmingen. Structure: Schlaich Bergermann and partner 1988 (© Jose L Fernandez Cabo).

Good schemes can be more complex. Ardant trusses, a combination of an arch with the rafters of classical roofs, competed against Polonceau trusses during the middle of the XIX century. Fig.29 shows an interesting example, containing the first laminated arch building in Europe (1964-65). The web is resolved using cast iron, timber and steel bars.

Figure 29: Roof of the German Gymnasium. London. UK. 1864-65 (© Jose L Fernandez Cabo).

Bowstrings, as in the example shown in Fig.30, are efficient structures when a proper slenderness, as is the case here, is used. Notice the use of steel rebar for the tie, a logical decision to resolve the joint at the springs. Web systems do not necessarily require so many elements. It is possible to solve this question with just some struts while using greater depth at the upper chord, as was shown in Fig.28.

Figure 30: Sport Hall, bowstring of 60m span made of timber and steel rebar (© Jose L Fernandez Cabo).

A roof needs cladding. The use of profiled steel sheeting for the cladding can also form the sub-structure, usually an arch or a even a shell (with more than one panel). Let us see two examples.

The first example is the new shed for Leuven train station (Fig.31).

Figure 31: New shed for Leuven train station, Belgium (© Jose L Fernandez Cabo).

The second, a humble roof, is shown in Fig. 32. Notice how the high depth of the steel plate with multiple folding (for local stability) is able to resolve an approx. 12 mspan with almost no other additional elements.

Figure 32: Multifunctional shed, Vicálvaro, Madrid (© Jose L Fernandez Cabo).

Complexity is present in many brilliant works. Fig. 33 and Fig. 34 show images of Santa Caterina market, Barcelona. The governing idea was to fold the roof and use coloured ceramic pieces as external cladding. This folded shape is incompatible with the structural scheme for a transversal medium span, and therefore the main arches do not follow the pattern of the roof (see Fig. 33). However, this is not finally a problem. The steel arches, which are pre-stressed at their ties, have good overall slenderness. The arch is built with a spatial truss whose depth resolves the secondary internal forces and gives overall stability.

Figure 33: Santa Caterina market, Barcelona, Spain. Architect: Enric Miralles; Engineering: José María Velasco, AMATRIA (© Jose L Fernandez Cabo (left); (© Joaquín Montón (right)).

Secondary beams follow a zigzag pattern (see Fig. 33 right and Fig. 34, left), which does not give rise to any problems. Only in some places, such as at the supports of the main façade (see Fig. 34, right), is the logic of the structure clearly violated. But the price paid there is small in comparison with the total cost.

Figure 34: Santa Caterina market, Barcelona, Spain. Architect: Enric Miralles; Structural Engineer: Jose María Velasco (© Jose L Fernandez Cabo).

Although a cheaper structure could obviously be built, this structure fits the architectural project, which is of particular interest, and offers a rational solution in its critical elements.

The results of Section 4 take neither general nor local stability into account. Tensile structures are selected in long spans, as the lack of any stability penalty notably reduces their dead load. Any suspension or cable-stay bridge is an example of this.

But even in short and medium spans, arches can modify their general scheme in order to address stability; as this is in fact the key problem for arches. Fig. 35 shows a now classical and highly efficient example, a Network arch. A tie with camber connected to the arch by a network of cables notably reduces the stability problem in the vertical plane. The transveral tilting of arches controls lateral stability.

Figure 35: Network arch walkway for the Anillo Verde near Fuente del Berro, Madrid (© Jose L Fernandez Cabo).

7 Conclusions

The dead load, maximum span and relative efficiency of a scheme with a particular slenderness can be computed easily. This is also the case for local buckling, assuming a certain mean penalty for compression members. Connections can easily increase theoretical values by from 10-20%; but it is not taken into account in the examples.

The results show that slenderness is the key geometrical parameter for controlling structural efficiency. The scheme, roughly speaking, is only crucial for a medium or long span; and in any case proper slenderness is still needed. This is not an obvious question at all.

Once good slenderness is achieved, the next step is simply to arrange the web system in angles of around 45 degrees with a horizontal line. This means that the higher the slenderness, the higher the number of elements connecting the chords.

The preliminary design of actual structures must include additional variables in its analysis and design: e.g. construction topics. The review of built structure makes it possible to place the exercise in a real context; showing how subtle and important managing the different variables can be. Simplicity is crucial. Techniques such as pre-stressing notably increase efficiency.

This article also presented architectural masterpieces built using short and medium spans, with structural schemes of poor efficiency. Any real problem is complex, and good solutions must take all of the variables into account. Although structural efficiency does not guarantee architectural success, both items are in fact compatible.

8 References

Aroca Hernández-Ros, Ricardo. 1989/1990. "Structure, Geometry and proportion". (Apuntes del Curso de Doctorado). *ETSAM, Madrid*. (Manuscript in Spanish).

Aroca Hernández-Ros, Ricardo. 1992/1993. "Structure, Geometry and proportion". (From a course for Ph. D students in Mexico). *ETSAM, Madrid*. (Manuscript in Spanish).

Aroca Hernández-Ros, Ricardo. 2002/2011. "Structures of minimum weight". Hand notes of the course La Estructura en el Proyecto Arquitectónico. *ETSAM, Madrid*. (Manuscripts in Spanish).

Fernandez Cabo, Jose L. 2012. *Matriz de equilibrio de estructuras trianguladas de barras articuladas con cargas en los nodos*. E.T.S. Arquitectura (UPM), Madrid. (in Spanish) `http://oa.upm.es/10742/`

MATALB®. MathWorks Co. http://www.mathworks.com MATALB®. MathWorks Co. http://www.mathworks.com

Maxwell, James Clerk. 1927 (1890) "On Reciprocal Figures, Frames and Diagrams of Forces". *Scientific Papers (From the Transactions of the R. S. of Edinburgh; Vol. XXVI; pp. 21-23); ed.; Paris*. Librarie Scientifique J. Hermann. pp. 161-177.

Michell, A.G.M. 1904. "The Limits of Economy of Material in Frame-Structures". *Philosophical Magazine.S.6*. Vol. 8; nº 47. Nov. pp. 589-597.

9 Appendix A script implemented in MATLAB® (release 2010).

```
    % The script firstly computes the internal forces of statically                %
% determinate 3D wire -frame pin -jointed structures with point loads at         %
% determinate 3D wire-frame pin-jointed structures with point loads at           %
% nodes by means of assembling the equilibrium matrix. Direction of              %
% restrains are limited to global axis.                                          %
% Quantity of material, optimum slenderness and maximum size are then            %
% derived                                                                        %
%--------------------------------------------------------------------------%
    clc     %clear command windows
    clear   %clear variables
%--------------------------------------------------------------------------%
% INPUT OF general data needed for initializing variables
%--------------------------------------------------------------------------%
    Num_Nod=3     % total number of nodes
    Num_Bar=3     % total number of elements or bars
    d=1           % auxiliary parameter, usually the total depth of the structure
    omega=1       % assumed buckling factor
%--------------------------------------------------------------------------%
% initialization of variables
%--------------------------------------------------------------------------%
    H_t=zeros(Num_Nod*3,Num_Bar); % equilibrium matrix without restrains
    Coor_Nod=zeros(Num_Nod,3);     % matrix with the coordinates of the nodes
    Coac_Nod=zeros(Num_Nod,3); % matrix with the restrains in global axis
    Coac_Nod=zeros(Num_Nod,3);  % matrix with the restrains in global axis

    Coac_Nod_Vec=zeros(Num_Nod*3,1);  % restrains in vector form
    Equil_List=1:1:Num_Nod*3;  % active Degrees of Freedom (DoF)
    Conec_Nod=zeros(Num_Bar,2); % Connectivitymatrix
    Conec_Nod=zeros(Num_Bar,2);  % Connectivity matrix
    Cos_Dir_Bar=zeros(4,Num_Bar);  % cosine directors and length of the members
    P_t=zeros(Num_Nod*3,1);  % nodal load vector without considering restrains
%--------------------------------------------------------------------------%
% INPUT of particular data
%--------------------------------------------------------------------------%
% nodal coordinates in global axis X,Y,Z
    Coor_Nod=[0,0,0; ...
              1,1,0; ...
              2,0,0]
% restrains in global axis X,Y,Z, 0= restrained, 1=free
    Coac_Nod=[0,0,0; ...
              1,1,0; ...
              1,0,0]
% connectivity matrix
    Conec_Nod=[1,2; ...
               1,3; ...
               2,3]
% nodal load vector without considering restrains
    P_t(5)=-1
%--------------------------------------------------------------------------%
% NO INPUT DATA ARE REQUIRED FROM HERE
%--------------------------------------------------------------------------%
%--------------------------------------------------------------------------%
% loading restrains in vector form
%--------------------------------------------------------------------------%
    for i=1:1:Num_Nod
```

```
    Coac_Nod_Vec(3*i-2)=Coac_Nod(i,1);
    Coac_Nod_Vec(3*i-1)=Coac_Nod(i,2);
    Coac_Nod_Vec(3*i)=Coac_Nod(i,3);
    end
% load the location of restraints in the vector List_Coac
    j=0;
    for i=1:1:Num_Nod*3
        if Coac_Nod_Vec(i)==0
          j=j+1;
          Coac_List(j)=i;
        end
    end
% active DoF where equilibrium is established
    Equil_List=setdiff(Equil_List,Coac_List) Equil_List=setdiff(Equil_List,Coac_List)
% cosine directors l,m,n in the first three rows, the fourth one is % used for the length
of the bar.
    for i=1:1:Num_Bar
    ini=Conec_Nod(i,1);
    fin=Conec_Nod(i,2);  % initial and final node of a bar
    Cos_Dir_Bar(4,i)=((Coor_Nod(fin,1)-Coor_Nod(ini,1))^ 2+(Coor_Nod(fin,2) ...
       -Coor_Nod(ini,2))^2+(Coor_Nod(fin,3)-Coor_Nod(ini,3))^ 2)^ 0.5;  %length
    Cos_Dir_Bar(1,i)=(Coor_Nod(fin,1)-Coor_Nod(ini,1))/Cos_Dir_Bar(4,i);
    Cos_Dir_Bar(2,i)=(Coor_Nod(fin,2)-Coor_Nod(ini,2))/Cos_Dir_Bar(4,i);
    Cos_Dir_Bar(3,i)=(Coor_Nod(fin,3)-Coor_Nod(ini,3))/Cos_Dir_Bar(4,i);
    end
    for j=1:1:Num_Bar
    ini=Conec_Nod(j,1);
    fin=Conec_Nod(j,2);  %initial and final node of a bar
    H_t(3*ini-2,j)=-Cos_Dir_Bar(1,j);
    H_t(3*ini-1,j)=-Cos_Dir_Bar(2,j);
    H_t(3*ini,j)=-Cos_Dir_Bar(3,j);
    H_t(3*fin-2,j)=Cos_Dir_Bar(1,j);
    H_t(3*fin-1,j)=Cos_Dir_Bar(2,j);
    H_t(3*fin,j)=Cos_Dir_Bar(3,j);
    end
%-----------------------------------------------------------%
    % Assemblage of equilibrium matrix considering now the restrains
%-----------------------------------------------------------%
    H=H_t(Equil_List,:);
    COND_H=cond(H)   % used to check if the matrix H were singular
%-----------------------------------------------------------%
% vector with nodal forces considering now the restrains
%-----------------------------------------------------------%
    P=P_t(Equil_List)
%-----------------------------------------------------------%
% solve the linear system of equations
%-----------------------------------------------------------%
    N=H\P;
%-----------------------------------------------------------%
% print the internal forces
%-----------------------------------------------------------%
    num=1:1:Num_Bar;
    esfuerzos=[num N]          % print displacements
%-----------------------------------------------------------%
% Compute the quantity of material, W, including the buckling if defined at previous
data
%-----------------------------------------------------------%
    N_w=N;
    for i=1:Num_Bar
```

```
        if N_w(i)<0
            N_w(i)=N_w(i)*omega;
        end
    end
    L=Cos_Dir_Bar(4,:);
    W=dot(L,abs(N_w))
%------------------------------------------------------------%
% Compute the components x,y,z of the quantity of material;
% Wx Wy and Wz respectively
%------------------------------------------------------------%
    Wx=0; Wy=0; Wz=0;
    for i=1:Num_Bar
        Wx=Wx+abs(L(i)*N(i)*Cos_Dir_Bar(1,i)^ 2);
        Wy=Wy+abs(L(i)*N(i)*Cos_Dir_Bar(2,i)^ 2);
        Wz=Wz+abs(L(i)*N(i)*Cos_Dir_Bar(3,i)^ 2);
    end
    Wx Wy Wz
%------------------------------------------------------------%
% Compute the Form Factor with and additional operation by the user
%------------------------------------------------------------%
    fact_esquema_k_2D=(Wx*Wy)^ 0.5
    disp( divide that value by the total load and by the span )
%------------------------------------------------------------%
% Compute the Optimal Slenderness with and additional operation by the user
%------------------------------------------------------------%
    esbelez_opt_2D=(Wy/Wx)^ 0.5
    disp( multiply that value by the current slenderness )
%------------------------------------------------------------%
% Draw structure (at its initial stage)
%------------------------------------------------------------%
    figure
    hold on
    for i=1:Num_Bar
        conect=Conec_Nod(i,:);
        xcoord = [Coor_Nod(conect(1),1)  Coor_Nod(conect(2),1)];
        ycoord = [Coor_Nod(conect(1),2)  Coor_Nod(conect(2),2)];
        zcoord = [Coor_Nod(conect(1),3)  Coor_Nod(conect(2),3)];
        line(xcoord,ycoord,zcoord);
    end
    axis  equal ; axis  tight ;
    axis([-1  (max(Coor_Nod(:,1))+1) -1   max(Coor_Nod(:,2))+1 -1 max(Coor_Nod(:,3))+1]);

    hold  off
    figure(gcf)
%%%%%%%%%%%%%%%%%%%%%%%%%%%%%%%%%%%%%%%%%%%%%%%%%%%%%%%%%%%%%%%%
% This Matlab code was written by Jose L Fernandez-Cabo, Department of      %
% Building Structures, Universidad Politécnica de Madrid, Avenida Juan de   %
% Herrera 4, 28040, Madrid.                                                 %
% Any comment can be sent to: jose.fcabo@upm.es                             %
% The theoretical basis can be viewed at http://oa.upm.es/10742/, even though %
% the document is in Spanish and the program is implemented in MAPLE.       %
% This code is intended for educational purposes.                           %
% Disclaimer:                                                               %
% The author reserves all rights but does not guarantee that the code is    %
% free from errors. Furthermore, he shall not be liable for any event       %
% caused by the use of the program.                                         %
%%%%%%%%%%%%%%%%%%%%%%%%%%%%%%%%%%%%%%%%%%%%%%%%%%%%%%%%%%%%%%%%
```